Electronic Supplementary Material (ESI) for Nanoscale.

Supplementary Information

Flexible Optical Limiters Based on Cu_3VSe_4 Nanocrystals

Xin-Ping Zhai,[a] Bo Ma, [a] Ming-Jun Xiao,[a] Wen Shang,[a] Zhi-Cong Zeng,[a] Qiang Wang,[a] and Hao-Li Zhang [a]**

[a] State Key Laboratory of Applied Organic Chemistry (SKLAOC), Key Laboratory of Advanced Catalysis of Gansu Province, College of Chemistry and Chemical Engineering, Key Laboratory of Special Function Materials and Structure Design, Ministry of Education, Lanzhou University, Lanzhou, 730000, China

Materials

Copper(I) chloride (CuCl), vanadyl acetylacetonate($VO(acac)_2$), Se powder, oleylamine (OLAM), oleic acid (OA), trioctylphosphine (TOP), trioctylphosphine oxide (TOPO), diphenyl ether and diphenyl diselenide was ordered from Aladdin Chemistry Co. Ltd. Toluene was purchased from Guangdong Fine Chemicals Engineering Technology Research Center Co., Ltd. Absolute ethyl alcohol (EtOH) was ordered LiAnLongBohua (Tianjin) Pharmaceutical& Chemical Co. Ltd.

Characterization

The Raman spectra were acquired using a confocal Raman Microscope System under excitation at 633 nm (Renishaw in via Raman microscope). The UV-Vis absorption spectra were collected on a TU-1810 Spectrophotometer (Beijing Purkinje General Instrument, China). Femtosecond transient absorption (TA) experiments were conducted on Helios transient absorption spectrometer (Ultrafast Systems), employing the regenerative amplifier (<110 fs, 1 kHz, 800 nm) (Coherent Legend Elite) as laser source seeded by a Coherent Chameleon oscillator (75 fs, 80 MHz). The supercontinuum white probe pulses at the range of 330-600 nm, 425-800 nm, and 850-1600 nm were generated on CaF_2, sapphire, and YAG crystals excited by the small portion 800-nm laser beam from the amplifier with appropriate beam intensity. The 350-nm pump pulses were generated from a Light Conversion OPerA-Solo optical parametric amplifier (285-2600 nm), and 400-nm pump pulses were generated from the main portion 800-nm laser beam through the SHG effect of the BBO crystal. To prevent the dipole-dipole interactions between the excited molecules and the probe light, the polarization of the pump and probe was set at the magic angle (54.7°) when 350-nm pump pulses as the pump beam. The

samples were stored in a 2-mm quartz cuvette for TA measurement at room temperature. The data analysis was conducted using Surface Xplore software that comes with Helios (Ultrafast Systems, LLC). The Z-scan data was collected by photodetectors under the irradiation of a 532-nm or 1064-nm laser beam with an FWHM of ~ 4 ns and a repetition rate of 10 Hz. The light source of fs Z-scan is the same as the pump light of the transient absorption spectrometer. The output fluence versus input fluence data was collected by the intensity-scan (I-scan) equipment system, and the equipment schematic diagram is shown in **Scheme S1**. The photos of the transmitted laser beam spot are taken by placing a ToupCam E3CMOS01200KPA digital camera after the sample in the I-scan device. The exposure time of the camera was 1500 ms and the gain was 500%. The spots are attenuated by passing through attenuators with the transmittance of 1% and 5% before entering the camera.

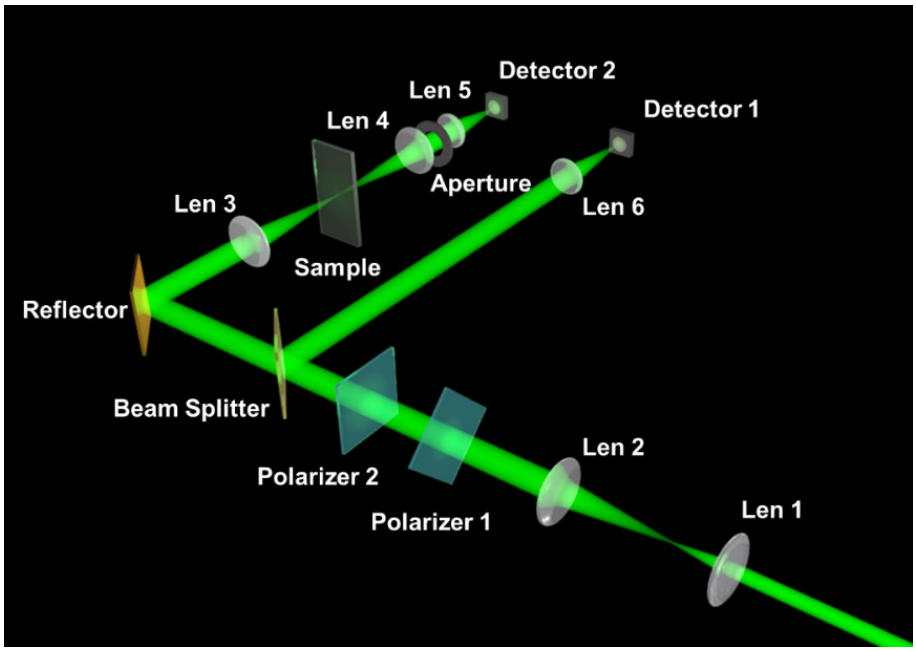

Scheme S1. The schematic diagram of I-scan system.

The TEM images were obtained by Talos F200S Field Emission Transmission Electron Microscopes (FEI, USA) at 200 kV. Powder X-ray diffraction (XRD) patterns of the samples

were obtained from a Panalypical X' Pert PRO diffractometer using Cu Kα X-rays between 5° and 90°. X-ray photoelectron spectroscopy (XPS) was performed on a Kratos AXIS Ultra DLD.

The numerically fitting of Z-scan curves

The Z-scan data were fitted to the nonlinear transmission equation using a sum of two nonlinear absorptions with opposite signs:

$$\alpha(I) = \frac{\alpha_0}{1 + \frac{I}{I_s}} + \beta I$$

where α(I) is the total nonlinear absorption coefficient, α0 is the linear absorption coefficient, β is the negative nonlinear absorption coefficient, I is the incident laser intensity, and Is is the saturation intensity, which is defined as the laser intensity at which α_0 drops to 50% of its initial value.

The imaginary part of the third-order nonlinear susceptibility associated with the nonlinear absorption coefficient β through:

$$Im\chi^{(3)}(esu) = {n^2c^2\beta}/{240\pi^2\omega} = {n^2\lambda\beta}/{0.158\pi}(cm/W)$$

Where n is the refractive index，c is the speed of light, ω is the optical angular frequency of the laser, and λ is the wavelength of the laser.

The band structure calculation

Computations were performed using first-principles density functional theory (DFT) methods based on the Vienna Ab-initio Simulation Package (VASP). The generalized gradient approximation (GGA) with the Perdew-Burke-Ernzerhof (PBE) functional was employed for high-precision optimization of the crystal structures. The convergence criteria for relaxation were set to a force threshold of less than 0.001 eV/Å and an energy threshold of less than 1×10^{-8} eV.

The plane-wave basis set was truncated at 500 eV and the k-point density was set to 6x6x6. After obtaining a fully converged geometry, the electronic structure was optimized using spin-orbit coupling (SOC) to calculate the material's band structure. The first Brillouin zone high-symmetry path of Γ-X-M-Γ was selected, and the Fermi level was used as the energy reference zero point by subtracting it from the energy.

1. The size distribution of the Cu_3VSe_4 NCs

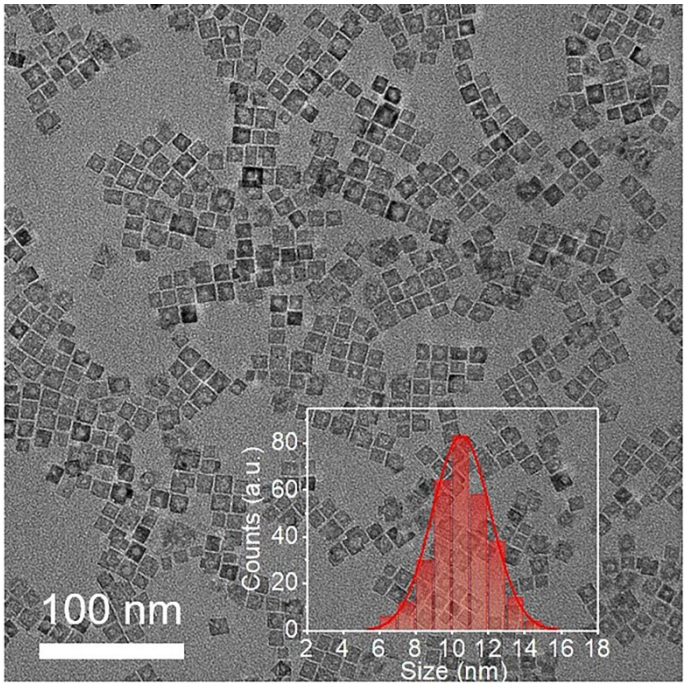

Figure S1 Representative TEM images of Cu_3VSe_4 NCs. Insets are the size distribution histograms.

2. HAADF-STEM image and EDX spectrum of Cu_3VSe_4 NCs.

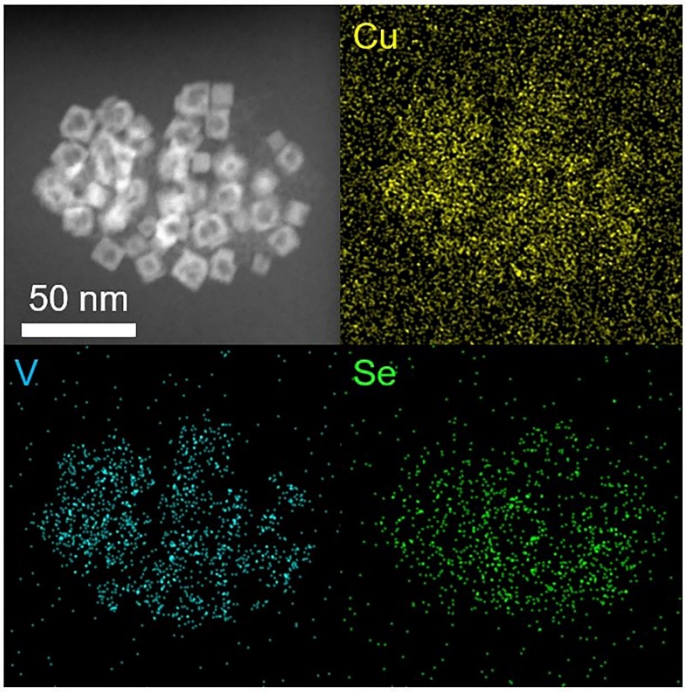

Figure S2 HAADF-STEM image and corresponding EDX mapping of Cu_3VSe_4 NCs.

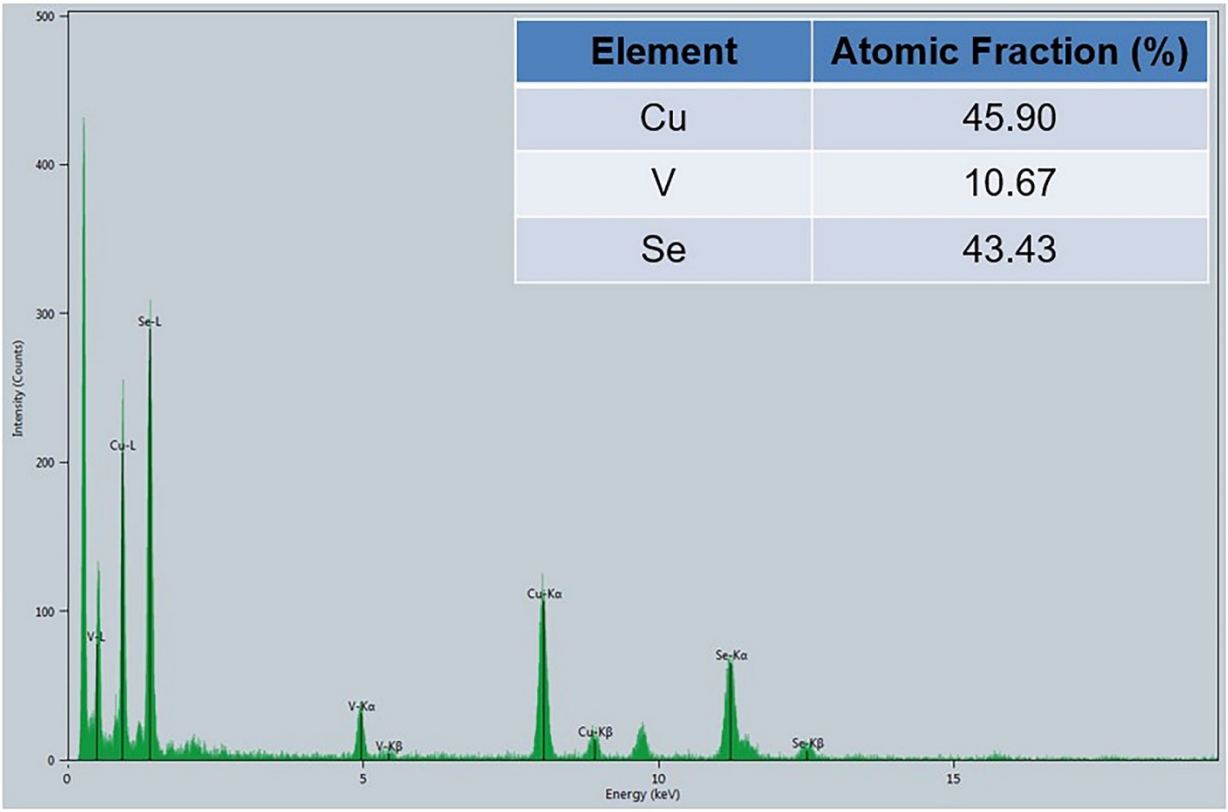

Figure S3 EDX spectrum of Cu_3VSe_4 NCs.

3. XPS survey spectra **of Cu_3VSe_4 NCs**

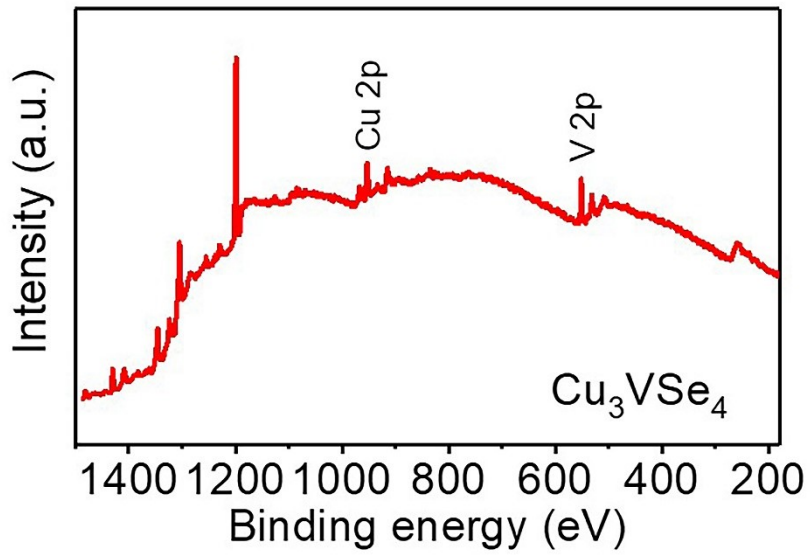

Figure S4. XPS survey spectra of Cu_3VSe_4 NCs.

4. Thermal stability of Cu_3VSe_4 NCs

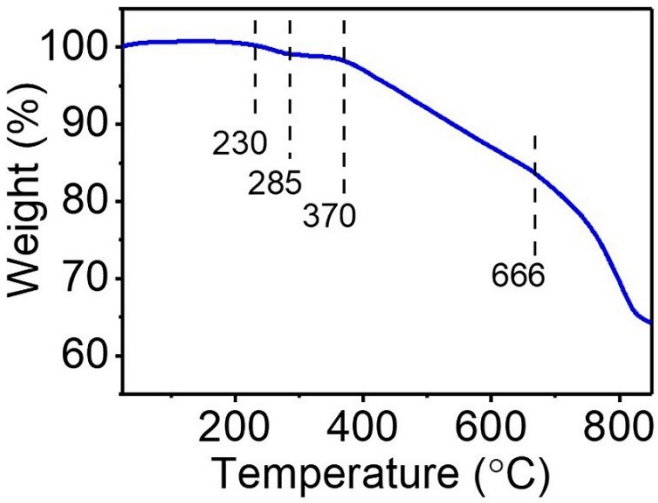

Figure S5 The thermogravimetric analysis (TGA) plot of Cu_3VSe_4 NCs. TGA was performed in the temperature interval 25-850 ℃ at a ramping rate of 20 ℃ min^{-1} under N_2 atmosphere.

5. Optical limiting properties of Cu_3VSe_4 NCs

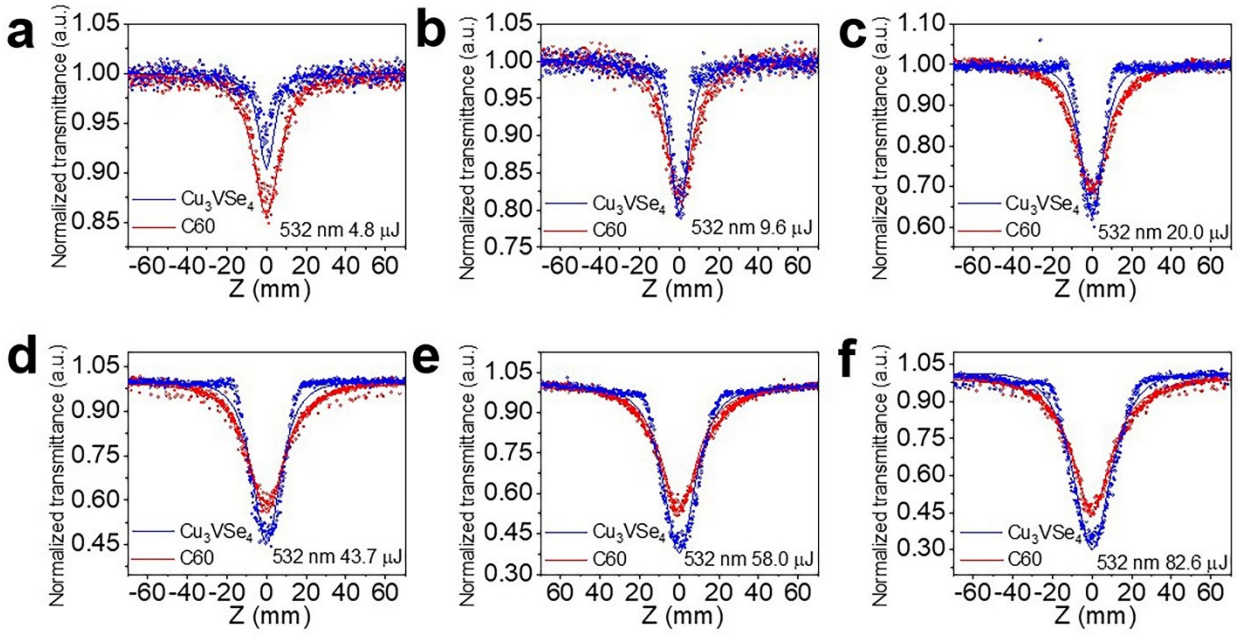

Figure S6 Open aperture ns Z-scan plots of Cu_3VSe_4 NCs and C60 solution in toluene at 532 nm under different energy.

Table S1 Summary of the fitted nonlinear optical parameters for the Cu_3VSe_4 NCs and C60 at 532 nm.

		4.8 μJ	9.6 μJ	20.0 μJ	43.7 μJ	58.0 μJ	82.6 μJ
Cu_3VSe_4	β (m/W)	4.30×10^{-10}	4.70×10^{-10}	5.10×10^{-10}	5.10×10^{-10}	5.50×10^{-10}	6.2×10^{-10}
	Is (W/m^2)	4.00×10^{11}	3.50×10^{11}	3.20×10^{11}	2.80×10^{11}	2.80×10^{11}	1.35×10^{11}
	Im$\chi^{(3)}$(esu)	1.03×10^{-11}	1.13×10^{-11}	1.22×10^{-11}	1.22×10^{-11}	1.32×10^{-11}	1.49×10^{-11}
C60	β (m/W)	5.90×10^{-10}	4.30×10^{-10}	4.30×10^{-10}	3.80×10^{-10}	3.30×10^{-10}	3.30×10^{-10}
	Is (W/m^2)	1.10×10^{12}	1.10×10^{12}	1.10×10^{12}	1.10×10^{12}	1.10×10^{12}	1.10×10^{12}
	Im$\chi^{(3)}$(esu)	1.41×10^{-11}	1.04×10^{-11}	1.03×10^{-11}	9.09×10^{-12}	7.92×10^{-12}	7.93×10^{-12}

Both the Cu_3VSe_4 NCs and C60 were dispersed in toluene with a linear transmittance of 0.7 at 532 nm.

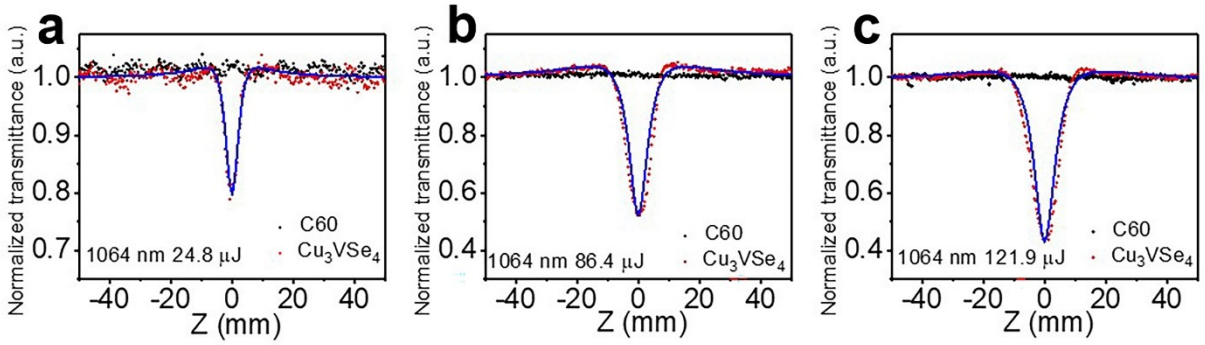

Figure S7 Open aperture ns Z-scan plots of Cu_3VSe_4 NCs and C60 solution at 1064 nm at different energy.

Table S2 Summary of the fitted nonlinear optical parameters for the Cu_3VSe_4 NCs at 1064 nm.

		24.8 μJ	86.4 μJ	121.9 μJ
Cu_3VSe_4	β (m/W)	1.51×10^{-10}	1.54×10^{-10}	1.60×10^{-10}
	Is (W/m^2)	2.50×10^{11}	1.40×10^{11}	1.60×10^{11}
	Im$\chi^{(3)}$(esu)	7.25×10^{-12}	7.39×10^{-12}	7.68×10^{-12}

The Cu_3VSe_4 NCs were dispersed in toluene with a linear transmittance of 0.78 at 1064 nm.

6. **Band gap of Cu_3VSe_4 NCs**

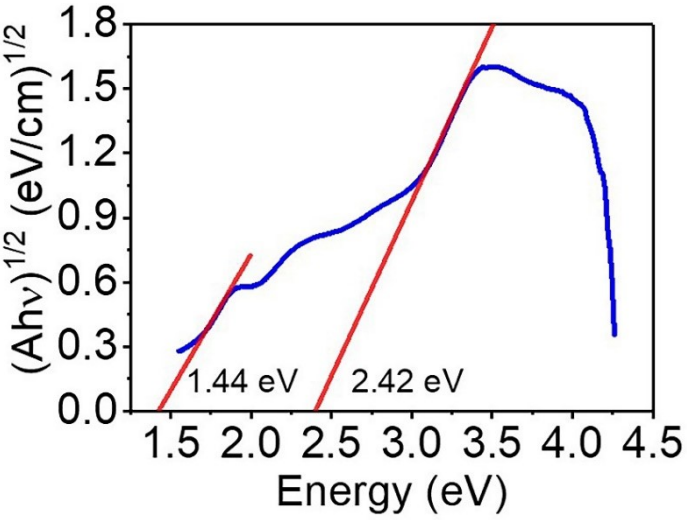

Figure S8 Band gaps of Cu_3VSe_4 NCs as disclosed by the UV-vis reflection spectra.

7. **Nonlinear refractive property of Cu_3VSe_4 NCs**

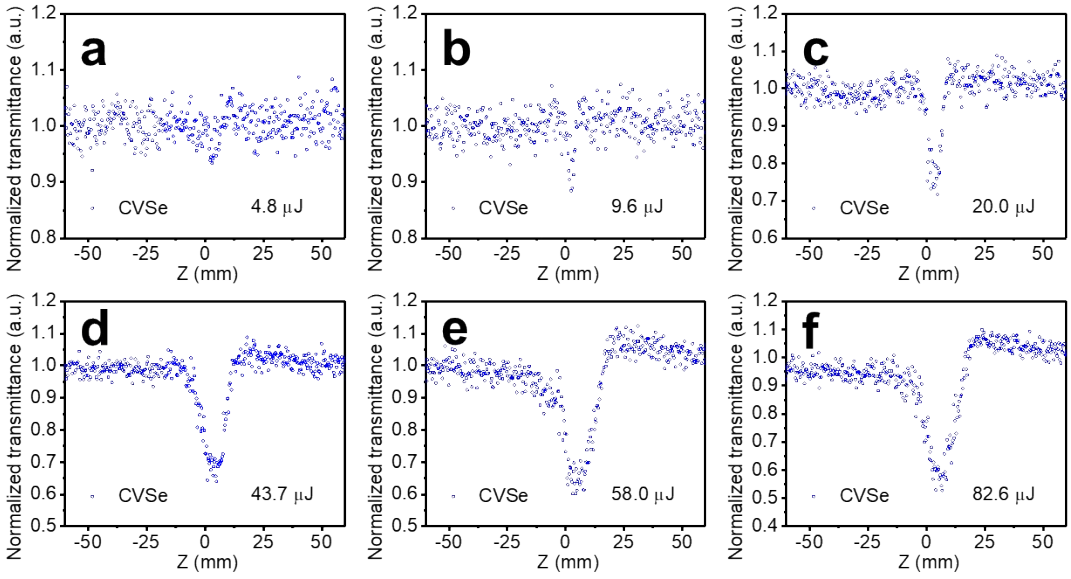

Figure S9 Dividing the normalized Z-scan data under the closed aperture by those under the open aperture gave the nonlinear refraction curves of the Cu_3VSe_4 NCs dispersed in toluene at 532 nm at different energy.

8. Fs Z-scan plots

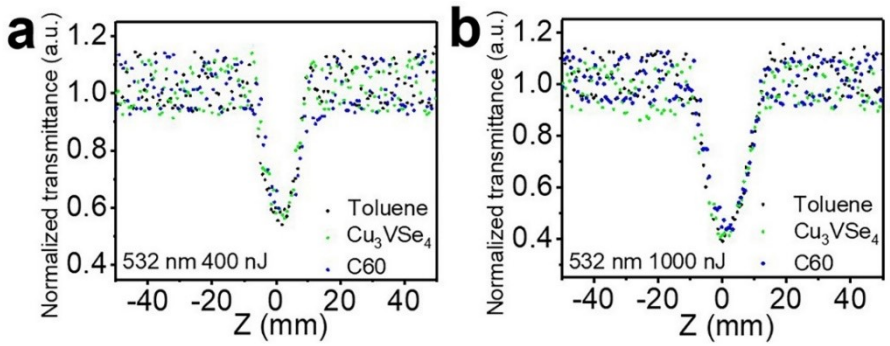

Figure S10 Open aperture fs Z-scan plots of Cu_3VSe_4 NCs and C60 solution in toluene at 532 nm at different energy. Both Cu_3VSe_4 NCs and C60 have no nonlinear optical response at 532 because the solution signal is no different from the solvent.

9. The calculation of the molar concentration of Cu_3VSe_4 NCs

We attempt to estimate the linear absorption cross-sections (σ) of Cu_3VSe_4 NCs from the excitation intensity dependent one-photon-induced GSB signals by using fs-TA spectroscopy. The GSB signal amplitude under different excitation intensities varies according to

$$-A\left(I/I_0\right) = -A_{max}\left[1 - e^{-\left(I/I_0\right)\cdot\sigma\cdot I_0}\right]$$

where $A\left(I/I_0\right)$ denotes the GSB signal amplitude of NCs after a long time delay as a function of excitation intensity, and I_0 is the minimum excitation intensity used in the fs-TA experiment.[1, 2]

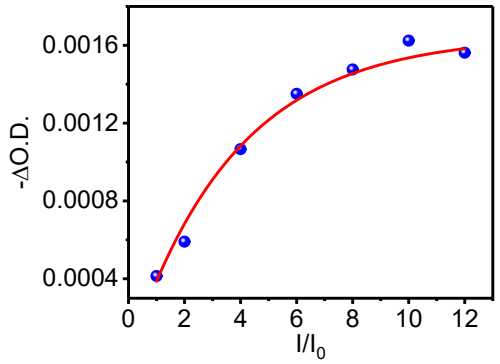

Figure S11 GSB signal amplitude at a time delay of 1 ns as a function of excitation intensity of Cu_3VSe_4 NCs. The curves are the best fitting lines based on the above equation.

As shown in **Figure S10**, the excitation intensity-dependent GSB signal amplitude at a delay time of 1 ns could be well-fitted with the above equation, from which the values of σ were extracted to be 5.41812×10^{-13} cm^2 for Cu_3VSe_4 NCs. Correspondingly, the values of molar distinction coefficients (ε) were determined to be $\varepsilon = \frac{\sigma \times N_A}{1000 \times (ln10)} = 1.42 \times 10^8$ $L\cdot cm^{-1}\cdot mol^{-1}$, where N_A is Avogadro's number. Additionally, the molar concentration of samples (Cm) can be determined by the equation $Cm = \frac{A}{\varepsilon \times L} = \frac{0.147}{1.42 \times 10^8 \times 1} = 1.035 \times 10^{-9}$ $mol\cdot L^{-1}$, where A is the absorbance of samples (A=0.147) and L is the thickness of samples (in the unit of cm, L=1 cm).

10. TA results of Cu_3VSe_4 NCs

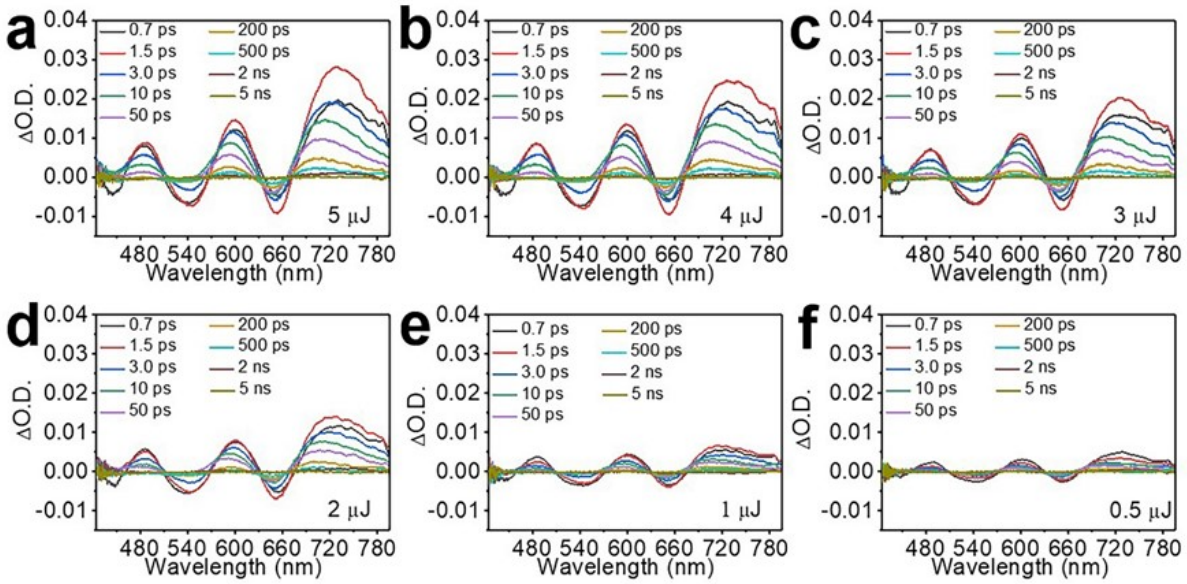

Figure S12 Representative spectra at different delay times for Cu_3VSe_4 NCs in the range of 0.7 ps to 5000 ps at pump energies of 5-0.5 μJ (a-f).

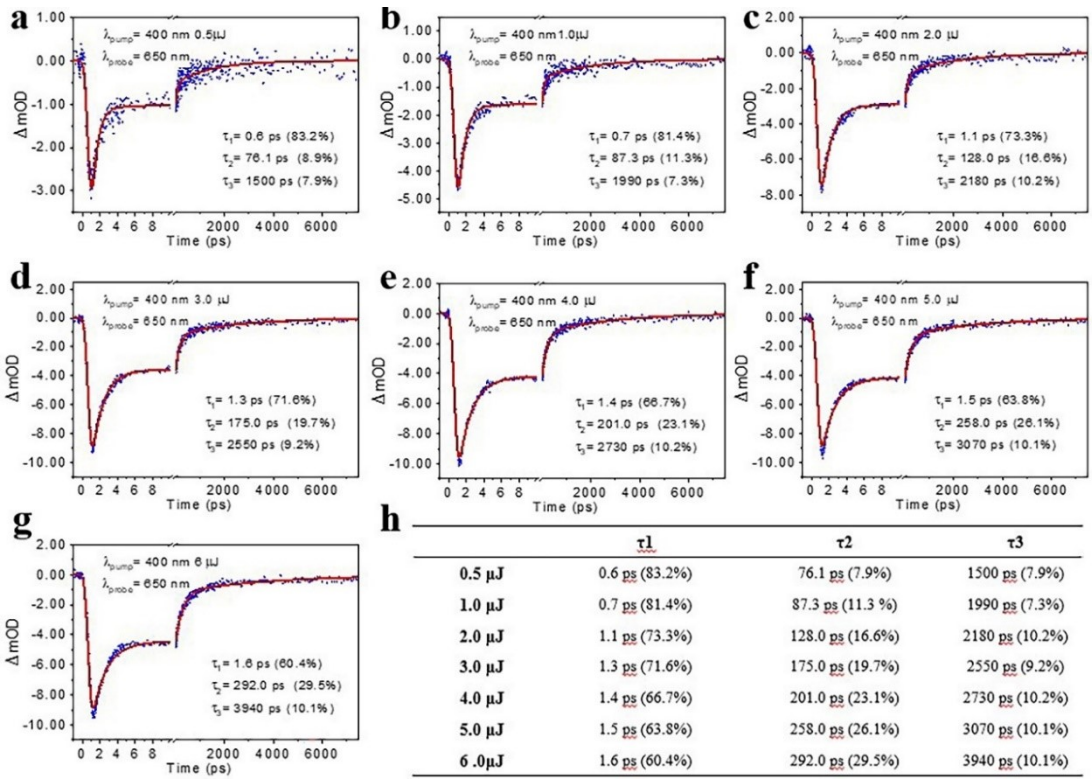

h

	τ1	τ2	τ3
0.5 μJ	0.6 ps (83.2%)	76.1 ps (7.9%)	1500 ps (7.9%)
1.0 μJ	0.7 ps (81.4%)	87.3 ps (11.3 %)	1990 ps (7.3%)
2.0 μJ	1.1 ps (73.3%)	128.0 ps (16.6%)	2180 ps (10.2%)
3.0 μJ	1.3 ps (71.6%)	175.0 ps (19.7%)	2550 ps (9.2%)
4.0 μJ	1.4 ps (66.7%)	201.0 ps (23.1%)	2730 ps (10.2%)
5.0 μJ	1.5 ps (63.8%)	258.0 ps (26.1%)	3070 ps (10.1%)
6 .0μJ	1.6 ps (60.4%)	292.0 ps (29.5%)	3940 ps (10.1%)

Figure S13 Representative decay curves of Cu_3VSe_4 NCs at probe of 650 nm under excitation at 400 nm with different pump energies of 0.5-6 μJ (a-g), and the summary of the lifetime (h).

11. TEM image, absorption spectrum and nonlinear absorption properties of the control-Cu_3VSe_4 NCs

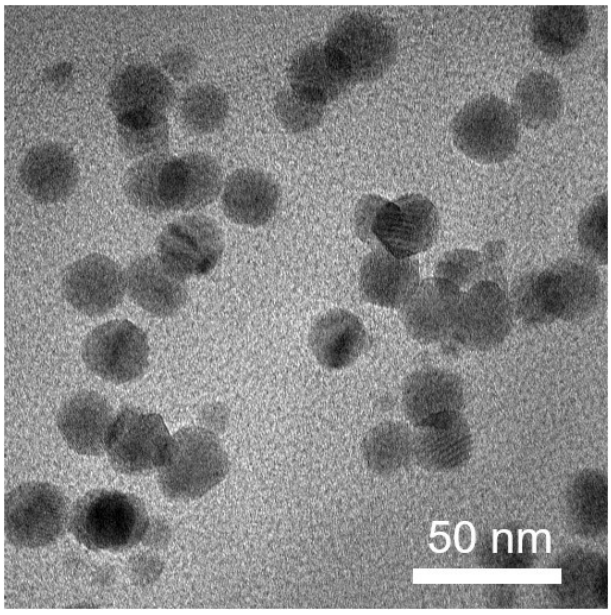

Figure S14 TEM image of the control-Cu_3VSe_4 NCs.

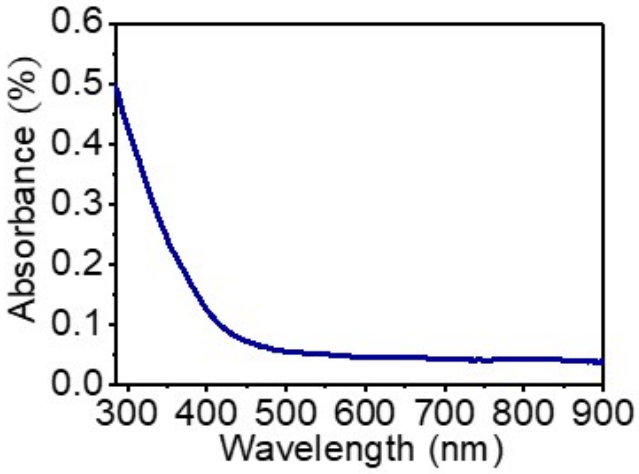

Figure S15 The absorption spectrum of the control-Cu_3VSe_4 NCs.

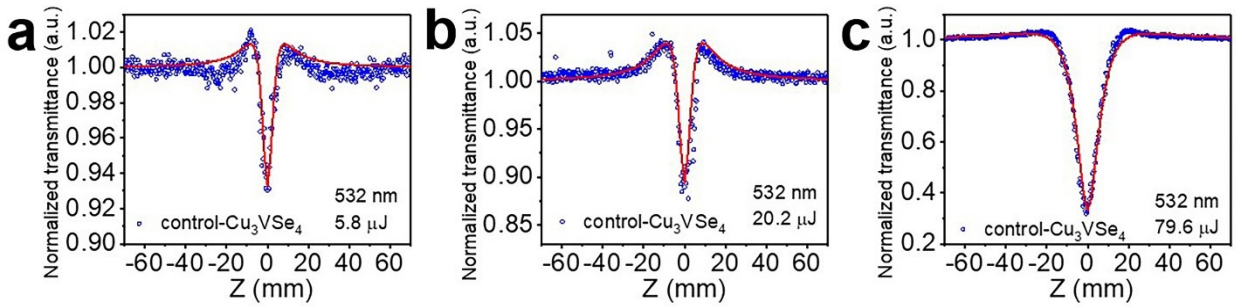

Figure S16 Open aperture Z-scan plots of the control-Cu_3VSe_4 NCs solution in toluene at 532 nm under different energies.

Table S3 Summary of the fitted nonlinear optical parameters for the control-Cu_3VSe_4 NCs.

		5.8 μJ	**20.2 μJ**	**79.6 μJ**
Cu_3VSe_4	**β (m/W)**	2.70×10^{-10}	1.20×10^{-10}	3.20×10^{-10}
	Is (W/m^2)	3.00×10^{11}	4.00×10^{11}	2.00×10^{11}

Table S4 Third- order nonlinear optical coefficients of selected materials with dielectric resonance.

Materials	Wavelength (nm)	β (m/W)	Refereces
Au/ITO	1450	-1.5×10^{-6}	ACS Nano 2022, 16, 8, 12878-12888
ITO	1550	-6.5×10^{-10}	Nanophotonics 2022; 11, 18, 4209-4219
Ag-SiO_2	500	-1.5×10^{-5}	ACS Photonics 2021, 8, 1, 125-129
TDBC	570	-5.4×10^{-7}	Adv.OpticalMater. 2018, 6, 1701400
ITO	1240	-3.4×10^{-8}	Science 2016, 352, 795
ZnO	1350	-3.3×10^{-10}	Phys. Rev. Lett. 2015, 116, 233901
Au film	550	2.7×10^{-9}	Nat.Commun. 2015, 6, 7757

12. Optical transmittance of epoxy resin film containing Cu_3VSe_4 NCs

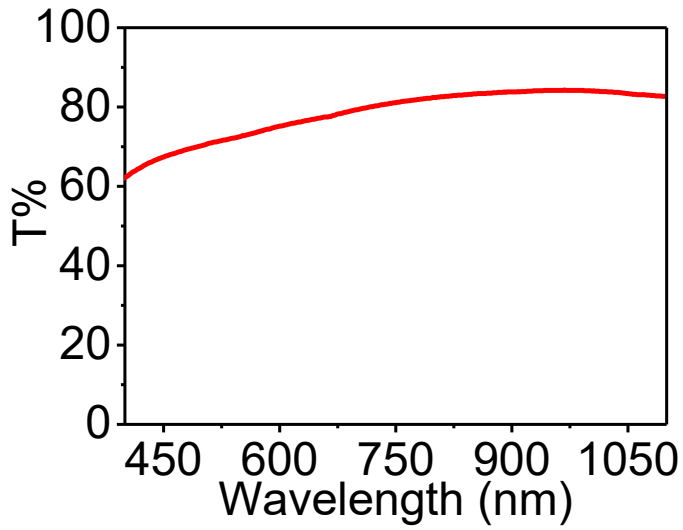

Figure S17 Transmission spectrum of the epoxy resin film containing Cu_3VSe_4 NCs.

13. Optical limiting properties of epoxy resin film containing Cu_3VSe_4 NCs after bending

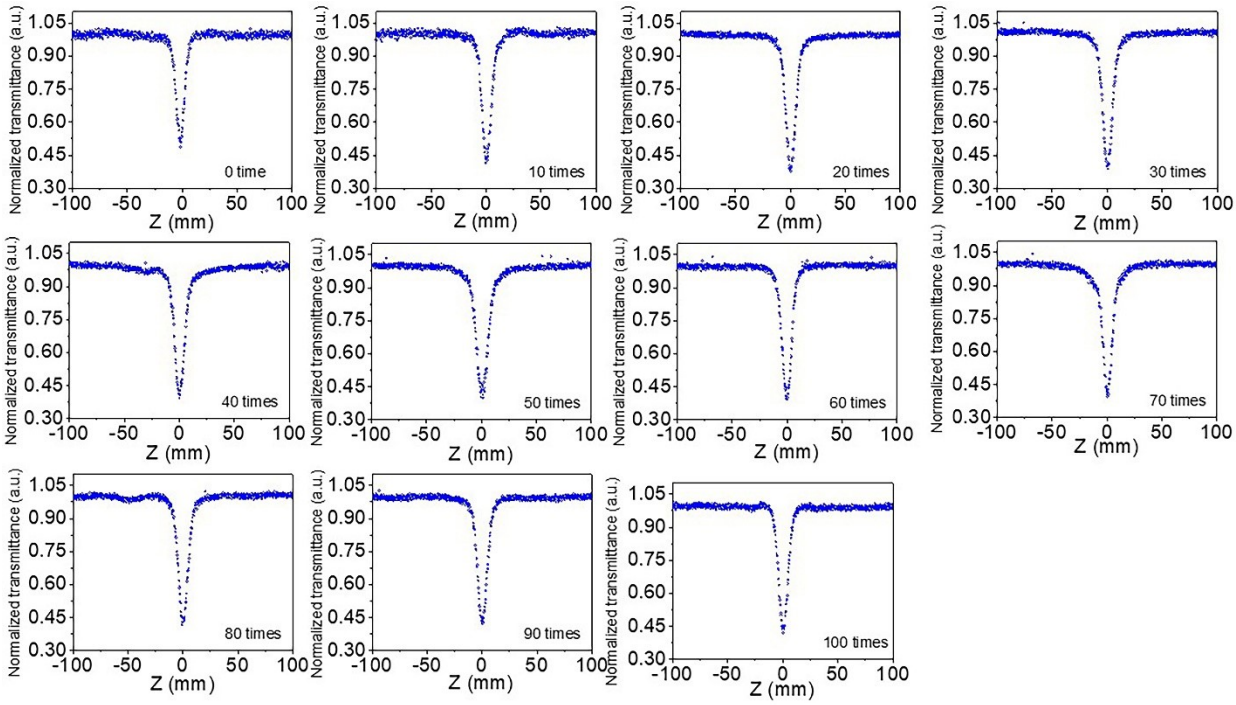

Figure S18 Open-aperture Z scan curves of the epoxy resin film containing Cu_3VSe_4 NCs after every 10 times of bending.

References

1. Chen, J.; Žídek, K.; Chábera, P.; Liu, D.; Cheng, P.; Nuuttila, L.; Al-Marri, M. J.; Lehtivuori, H.; Messing, M. E.; Han, K.; Zheng, K.; Pullerits, T., Size- and Wavelength-Dependent Two-Photon Absorption Cross-Section of $CsPbBr_3$ Perovskite Quantum Dots. *J. Phys. Chem. Lett.* **2017,** *8* (10), 2316-2321.
2. He, T.; Li, J.; Qiu, X.; Xiao, S.; Yin, C.; Lin, X., Highly Enhanced Normalized-Volume Multiphoton Absorption in $CsPbBr_3$ 2D Nanoplates. *Adv. Opt. Mater.* **2018,** *6* (21), 1800843.